Relevance of the light line in planar photonic crystal waveguides with weak vertical confinement

P. Kaspar,[1,*] R. Kappeler,[1] D. Erni,[2] and H. Jäckel[1]

[1]*Electronics Laboratory, ETH Zurich, CH-8092 Zürich, Switzerland*
[2]*General and Theoretical Electrical Engineering (ATE), Faculty of Engineering, University of Duisburg-Essen, and CeNIDE - Center for Nanointegration Duisburg-Essen, D-47048 Duisburg, Germany*

[*]*kaspar@ife.ee.ethz.ch*

Abstract: The concept of the so-called light line is a useful tool to distinguish between guided and non-guided modes in dielectric slab waveguides. Also for more complicated structures with 2D mode confinement, the light lines can often be used to divide a dispersion diagram into a region of a non-guided continuum of modes, a region of discrete guided modes and a forbidden region, where no propagating modes can exist. However, whether or not the light line is a concept of practical relevance depends on the geometry of the structure. This fact is sometimes ignored. For instance, in the literature on photonic crystal waveguides, it is often argued that substrate-type photonic crystal waveguides with a weak vertical confinement are inherently lossy, since the entire bandgap including the line defect modes is typically located above the light line of the substrate. The purpose of this article is to illustrate that this argument is inaccurate and to provide guidelines on how an improved light line concept can be constructed.

OCIS codes: (230.7370) Waveguides; (130.5296) Photonic crystal waveguides; (130.3120) Integrated optics devices.

References and links

1. L. V. Hau, S. E. Harris, Z. Dutton, and C. H. Behroozi, "Light speed reduction to 17 metres per second in an ultracold atomic gas," Nature **397**, 594–598 (1999).
2. S. Mahnkopf, M. Kamp, A. Forchel, and R. März, "Tunable distributed feedback laser with photonic crystal mirrors," Appl. Phys. Lett. **82**, 2942–2944 (2003).
3. O. Painter, R. K. Lee, A. Scherer, A. Yariv, J. D. O'Brien, P. D. Dapkus, and I. Kim, "Two-dimensional photonic band-gap defect mode laser," Science **284**, 1819–1821 (1999).
4. B. Corcoran, C. Monat, C. Grillet, D. J. Moss, B. J. Eggleton, T. P. White, L. O'Faolain, and T. F. Krauss, "Green light emission in silicon through slow-light enhanced third-harmonic generation in photonic-crystal waveguides," Nat. Photonics **3**, 206–210 (2009).
5. Y. Akahane, T. Asano, B.-S. Song, and S. Noda, "High-Q photonic nanocavity in a two-dimensional photonic crystal," Nature **425**, 944–947 (2003).
6. T. Tanabe, M. Notomi, E. Kuramochi, A. Shinya, and H. Taniyama, "Trapping and delaying photons for one nanosecond in an ultrasmall high-Q photonic-crystal nanocavity," Nat. Photonics **1**, 49–52 (2007).
7. H. Gersen, T. J. Karle, R. J. P. Engelen, W. Bogaerts, J. P. Korterik, N. F. van Hulst, T. F. Krauss, and L. Kuipers, "Real-space observation of ultraslow light in photonic crystal waveguides," Phys. Rev. Lett. **94**, 073903 (2005).
8. Y. A. Vlasov, M. O'Boyle, H. F. Hamann, and S. J. McNab, "Active control of slow light on a chip with photonic crystal waveguides," Nature **438**, 65–69 (2005).

#153125 - $15.00 USD Received 18 Aug 2011; revised 4 Nov 2011; accepted 4 Nov 2011; published 14 Nov 2011

9. S. Hughes, L. Ramunno, J. F. Young, and J. E. Sipe, "Extrinsic optical scattering loss in photonic crystal waveguides: Role of fabrication disorder and photon group velocity," Phys. Rev. Lett. **94**, 033903 (2005).
10. L. O'Faolain, S. A. Schulz, D. M. Beggs, T. P. White, M. Spasenović, L. Kuipers, F. Morichetti, A. Melloni, S. Mazoyer, J. P. Hugonin, P. Lalanne, and T. F. Krauss, "Loss engineered slow light waveguides," Opt. Express **18**, 27627–27638 (2010).
11. Let σ_y denote a reflection in the *x*-*z* plane, i.e., $\sigma_y\hat{\mathbf{x}} = \hat{\mathbf{x}}$, $\sigma_y\hat{\mathbf{y}} = -\hat{\mathbf{y}}$, $\sigma_y\hat{\mathbf{z}} = \hat{\mathbf{z}}$ for the unit vectors $\hat{\mathbf{x}}$, $\hat{\mathbf{y}}$, and $\hat{\mathbf{z}}$, respectively. **E** transforms like a vector, whereas **H** transforms like a pseudovector under an orientation-reversing map. A mode of even parity is characterized by $\mathbf{E}(\sigma_y\mathbf{r}) = \sigma_y\mathbf{E}(\mathbf{r})$ and $\mathbf{H}(\sigma_y\mathbf{r}) = -\sigma_y\mathbf{H}(\mathbf{r})$, a mode of odd parity by $\mathbf{E}(\sigma_y\mathbf{r}) = -\sigma_y\mathbf{E}(\mathbf{r})$ and $\mathbf{H}(\sigma_y\mathbf{r}) = \sigma_y\mathbf{H}(\mathbf{r})$. Note that different conventions of parity might be used in other contexts.
12. Z. Zhu and T. G. Brown, "Full-vectorial finite-difference analysis of microstructured optical fibers," Opt. Express **10**, 853–864 (2002).
13. R. März, *Integrated Optics: Design and Modeling* (Artech House, Norwood, 1995).
14. It might be interesting to note that the condition of Eq. (1) for guided modes can be proven by a rigorous mathematical analysis, as long as there is a radius R around the core, for which $n(\mathbf{r}) = n_\infty$ holds for all $\mathbf{r} \in \mathbb{R}^2$ with $|\mathbf{r}| > R$ [A.-S. Bonnet-Ben Dhia and P. Joly, "Mathematical analysis and numerical approximation of optical waveguides," in *Mathematical Modeling in Optical Science*, G. Bao, L. Cowsar, and W. Masters, eds. (Siam, Philadelphia, 2001), pp. 273–324, Frontiers in Applied Mathematics]. In other words, Eq. (1) holds for all guided modes, if outside of a circle of radius R the background is made up of a homogeneous medium of refractive index n_∞. This condition is not fulfilled by the structure of Fig. 1 if we let $h_{\text{bot}} \to \infty$.
15. D. Marcuse, *Theory of Dielectric Optical Waveguides*, Quantum Electronics: Principles and Applications (Academic Press, Boston, 1991), 2nd ed.
16. T. A. Birks, P. J. Roberts, P. S. J. Russell, D. M. Atkin, and T. J. Shepherd, "Full 2-D photonic bandgaps in silica/air structures," Electron. Lett. **31**, 1941–1943 (1995).
17. J. C. Knight, J. Broeng, T. A. Birks, and P. S. J. Russell, "Photonic band gap guidance in optical fibers," Science **282**, 1476–1478 (1998).
18. S. G. Johnson, S. Fan, P. R. Villeneuve, J. D. Joannopoulos, and L. A. Kolodziejski, "Guided modes in photonic crystal slabs," Phys. Rev. B **60**, 5751–5758 (1999).
19. S. G. Johnson and J. D. Joannopoulos, "Block-iterative frequency-domain methods for Maxwell's equations in a planewave basis," Opt. Express **8**, 173–190 (2001).
20. B. Lombardet, L. A. Dunbar, R. Ferrini, and R. Houdré, "Fourier analysis of Bloch wave propagation in photonic crystals," J. Opt. Soc. Am. B **22**, 1179–1190 (2005).
21. W. Kuang and J. D. O'Brien, "Reducing the out-of-plane radiation loss of photonic crystal waveguides on high-index substrates," Opt. Lett. **29**, 860–862 (2004).

1. Introduction

Line defect planar photonic crystal (PhC) waveguides have become popular in the context of slow light applications. The general interest in slow light was boosted by the demonstration of extreme slow-down factors in a Bose Einstein condensate [1] and by rapid advances made in PhC fabrication technology, which led to the experimental verification of various photonic bandgap effects, such as PhC mirrors [2, 3], the enhancement of nonlinear effects [4], high-Q cavities [5, 6], and slow light in PhC waveguides [7, 8], to mention but a few. One of the main challenges faced by PhC-based waveguide applications is the optical propagation loss, which is particularly pronounced in slow-light operation [9, 10], and in the case of structures with a weak refractive index contrast between the planar waveguide layers. Several arguments have been put forward to explain the difference in loss between substrate-type (low index contrast) and membrane-type (high index contrast) structures. One of them is based on the so-called "light line" concept: membrane-type PhC waveguides can be easily designed to have line defect modes below the light line of the cladding (e.g. air), whereas in the first Brillouin zone of substrate-type structures the entire bandgap is typically situated above the light line of the substrate. This observation is used to imply that there are no "truly" guided line defect modes of the substrate-type PhC waveguide, whereas the membrane-type structure naturally exhibits guided modes (theoretically loss-free). However, there is a flaw in this line of arguments, which can be boiled down to the fact that the geometry for lateral confinement is not taken into account when the light line concept is applied in a too simplistic manner. It is the purpose of this article

#153125 - $15.00 USD Received 18 Aug 2011; revised 4 Nov 2011; accepted 4 Nov 2011; published 14 Nov 2011

to substantiate this statement and to replace the light line argument by a more accurate model to predict the separatrix between high-loss and low-loss modes in a dispersion diagram. We believe that, in the past, over-stressing the light line concept has caused many workers in the field to reject substrate-type PhC waveguides in general for being a fundamentally ill-suited workhorse. We intend to demonstrate that this might have been unjustified.

The article is organized as follows. First, a buried rectangular waveguide (BRWG) is investigated, which resembles a deeply etched planar PhC waveguide in terms of geometry of the cross-section. No periodic dielectric modulation is considered in this section (Sec. 2.1). The dispersion diagram of the BRWG is analyzed in detail with respect to the separatrix that marks the boundary between guided and non-guided modes. Then, the insights gained from the BRWG are applied to PhC waveguide structures in Sec. 3.1. It is shown that there is some more design freedom for substrate-type PhC waveguides than expected up to date. Section 3.2 gives an outlook on how this new design freedom might be exploited to find a substrate-type PhC waveguide design, which does not exhibit inherent radiation losses. Finally, a few conclusive remarks are made in Sec. 4

2. The background line concept

2.1. The buried rectangular waveguide

We consider the structure shown in Fig. 1(a) and refer to it as the buried rectangular waveguide. All materials are non-absorbing and their refractive indices are indicated in the figure. The simulated dispersion diagram of the waveguide is shown in Fig. 1(b), along with the dispersion lines of homogeneous materials for each of the refractive indices present in the structure. We show the fundamental modes of odd parity [11] with respect to the *x*-*z* mirror plane ($E_x = H_y = E_z = 0$ in the symmetry plane), computed by Lumerical (bullets), a commercially available 2D finite difference frequency domain (FDFD) eigenmode solver [12]. The simulation domain is terminated by a perfectly matched layer (PML). For large propagation constants ($k_x \to \infty$), the waveguide mode crosses the dispersion line of the substrate (n_2) and converges (not shown here) to the dispersion line of the core (n_1). For small propagation constants, a cutoff is found near an effective refractive index of 2.6. This observation requires explanation, since it contradicts a widespread understanding of how the waveguiding mechanism works. Conventional wisdom has it that the effective refractive index lies between the core index and the largest index of the materials involved in the guiding action. Formally, this translates into the statement that all guided modes of a longitudinally invariant dielectric waveguide must satisfy the condition [13]

$$\max_{\mathbf{r}\in\mathbb{R}^2} n(\mathbf{r}) > n_{\text{eff}} > \max_{\mathbf{r}\in\partial\mathbb{R}^2} n(\mathbf{r}), \tag{1}$$

where $\partial\mathbb{R}^2$ is the "boundary at infinity" of the cross-section $\mathbb{R}^2$ of the waveguide. The condition is based on the definition of guided modes, i.e., on the prerequisite that all fields decay exponentially and no oscillatory fields shall be supported at infinite distances from the core. For our BRWG, Eq. (1) writes as $n_1 = 3.33 > n_{\text{eff}} > n_2 = 3.15$, which is in clear disagreement with those results of Fig. 1 which are located above the dispersion line of the substrate.

To analyze the discrepancy between our simulation and Eq. (1), it has to be verified whether the modes under question can qualify as guided modes. In the strict sense, the fields of a guided mode decay exponentially at infinite distances from the waveguide core. Numerically, this criterion is hard to assess in a rigorous manner. The classification is generally done based on the amount of energy in the PML surrounding the computational domain, using some arbitrary threshold. Figure 2 shows the propagation loss introduced to the BRWG of Fig. 1 by the PML. Four different sizes of h_{bot} are considered, while h_{top} is kept constant at 1 μm. The four curves correspond to h_{bot} values of 2 μm, 4 μm, 6 μm, and 8 μm. The size of the simulation

#153125 - $15.00 USD Received 18 Aug 2011; revised 4 Nov 2011; accepted 4 Nov 2011; published 14 Nov 2011

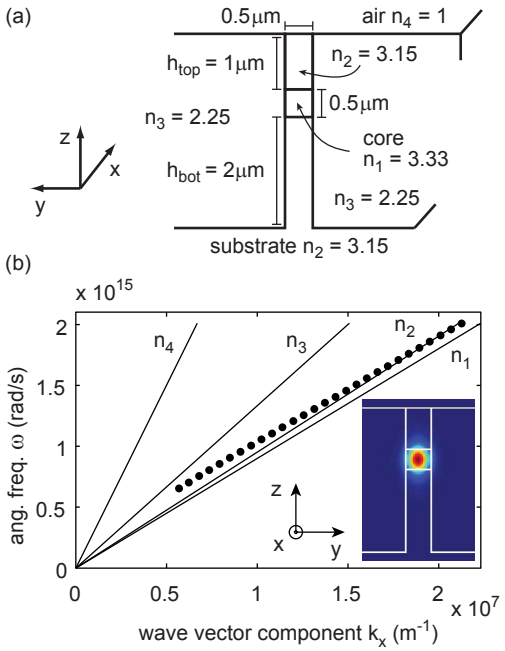

Fig. 1. (a) Schematic structure of a buried rectangular waveguide; (b) Dispersion diagram $\omega(k_x)$. The solid lines are the dispersion lines of the materials present in the structure, labeled with their respective refractive index. The waveguide modes (bullets) are computed by Lumerical in a range between 0.9 and 3.0 μm (= cutoff). The inset shows the field intensity $|\mathbf{E}|^2$ distribution of a mode with an effective refractive index of $n_{\text{eff}} = 3.0$; the field intensity is scaled from blue (low) to red (high).

domain ($16 \times 16\,\mu$m) and the mesh resolution (grid spacing between 40 nm, in the core, and 80 nm, far from the core) are the same for all curves. The PML loss near cutoff is substantial for $h_{\text{bot}} = 2\,\mu$m, but is drastically reduced for the larger values of h_{bot}. The limit of numerical accuracy is reached around 10^{-10} dB/cm. It is interesting to note that if the position of the PML is moved further away from the waveguide core, the change in PML loss is negligible. For instance, with $h_{\text{bot}} = 4\,\mu$m and a frequency of 140 THz ($n_{\text{eff}} = 2.8$), the PML loss fluctuates by $\pm\,0.0041\,\%$ when we vary the position of the lower PML boundary in a range that spans 10 μm (95 % confidence interval from a set of 32 data points). This indicates that the main contribution to the PML loss is given by an oscillatory field rather than an exponentially decaying one. In this respect, we cannot classify the modes as guided modes. Nevertheless, the results of Fig. 2 suggest that arbitrarily low PML losses can be obtained by increasing h_{bot} to infinity. We conclude that, for a BRWG with $h_{\text{bot}} \to \infty$, guided modes exist with effective refractive indices outside the range given in Eq. (1).

In order to understand why the condition of Eq. (1) is violated for the guided modes of the BRWG with $h_{\text{bot}} \to \infty$, we have to go back to the prerequisites from which the condition follows. As indicated above, Eq. (1) is based on the requirement that the dielectric "background" at infinity must not support any oscillating solutions of Maxwell's equations. For simplicity, we will let $h_{\text{top}} \to \infty$, as well. The background at infinity of this system is composed of the materials of refractive indices n_2 (thin slab) and n_3 (two half-spaces), i.e., it is essentially a slab waveguide structure [14]. The oscillating modes of a slab waveguide are either guided modes or radiation modes of the slab, and they can be computed analytically [15]. There is no oscillating mode

#153125 - $15.00 USD Received 18 Aug 2011; revised 4 Nov 2011; accepted 4 Nov 2011; published 14 Nov 2011

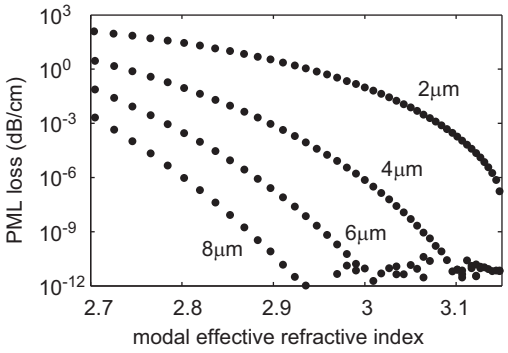

Fig. 2. Simulated optical loss in the PML around the structure of Fig. 1(a) as a function of modal effective refractive index. The four curves correspond to different values of h_{bot}: $2\,\mu$m, $4\,\mu$m, $6\,\mu$m, $8\,\mu$m. Around a loss of 10^{-10} dB/cm, the limit of numerical accuracy of the simulation is reached. In this range, some points with a negative result occur; they are omitted from the plot.

of the slab with refractive index $n_{\mathrm{eff}} = n_2$. Therefore, the dispersion line of the substrate (n_2) cannot be relevant in the determination of the BRWG cutoff. Instead, the relevant separatrix in the dispersion diagram, which separates guided from non-guided modes, is the dispersion curve of the fundamental mode of the background system (the $n_3/n_2/n_3$ slab waveguide). We will refer to this separatrix as the "background line". Propagating modes of the full BRWG system, which are located below the background line are guided modes and theoretically loss-free.

As a further validation of our background line concept, Fig. 3 shows the cutoff of the BRWG of Fig. 1 together with the background line. Depending on the parity (w.r.t. the *x*-*z* symmetry plane) in the core of the BRWG fundamental mode (bullets), the TE or TM modes of the background slab waveguide have to be considered (solid lines). The simulation of the BRWG is again performed with the Lumerical mode solver, and the results of odd parity correspond to those of Fig. 1(b). The background lines are calculated from analytical equations [15]. Cutoff for both parities occurs as predicted. This confirms that the background line bears more practical relevance than the condition of Eq. (1) (dotted vertical line in Fig. 3) if h_{bot} is large.

Here, the background line was motivated from first principles. However, there are a few cases in the literature, where the concept was implicitly used. In the context of holey fibers, the band diagram of a 2D PhC structure is projected onto the out-of-plane axis [16] and the gaps appearing in this way are exploited for low-loss light propagation [17]. Furthermore, the *effective index method*, which is a popular analytical approximation to find the modes of integrated optical waveguides (such as ridge waveguides), makes use of the background modes as one of the steps in the simplification procedure for an analytical mode analysis. It is important to note that, while the effective index method makes considerable errors in determining the dispersion near cutoff of certain waveguides, the cutoff itself is always predicted on the correct separatrix in the dispersion diagram (but not at the correct location on the separatrix).

The background line cannot predict the cutoff frequency of a given waveguide structure; it only represents the separatrix in the dispersion diagram on which the cutoff is to be expected. Therefore, it seems legitimate to ask of what practical use it might be. The answer is simple: it is useful, whenever we compute the dispersion diagram of a waveguide numerically with a method that doesn't easily allow us to distinguish between guided and non-guided modes. A prominent example is a dispersion diagram of a photonic crystal (PhC) waveguide computed

#153125 - $15.00 USD Received 18 Aug 2011; revised 4 Nov 2011; accepted 4 Nov 2011; published 14 Nov 2011

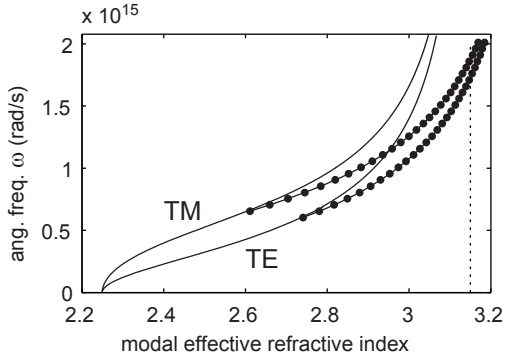

Fig. 3. Illustration of mode cutoff for the BRWG depicted in Fig. 1(a). The bullets are the numerical mode solver results for the two parities. The solid lines represent the TE and TM fundamental mode of the background slab waveguide, as indicated in the graph. The dashed vertical line indicates the dispersion line of the substrate material.

with the plane wave expansion method.

2.2. The role of total internal reflection

It is a widespread misconception that the condition of Eq. (1) follows directly from the law of total internal reflection when considering the interface of a waveguide core with the surrounding material of highest refractive index. In our case of the BRWG, this would mean that at the lower interface between the core and the substrate material total internal reflection dictates the cutoff behavior of the structure. However, this reasoning contains two errors at a time. Firstly, the condition of total internal reflection cannot be represented simply as a line in a dispersion diagram. This works in a 1D system, where mode confinement occurs only in one direction, but not for systems with 2D mode confinement. Secondly, it is wrong to assume that the loss of total internal reflection is responsible for mode cutoff in waveguides with a 2D mode confinement. This is treated in detail by Marcuse [15] for the case of weakly guiding optical fibers with a circular cross-section. Analytical solutions of the fiber are derived, for which it is shown that loss of total internal reflection does not yet occur at the cutoff point.

3. Substrate-type photonic crystal waveguides

In the photonic crystal community, the condition of Eq. (1) is often referred to as the “light line” or “light cone” concept. For instance, the light cone helps to interpret numerically computed band diagrams of 2D-periodic systems, which are not uniform in the third dimension. Two examples of such a system are depicted schematically in Fig. 4. They are 2D-periodic arrays of holes etched into a slab waveguide. To analyze the system of Fig. 4(a), the band diagram is computed for 3D unit cells, and then it is overlaid with the light cone of the surrounding homogeneous material in order to retain only the guided modes of the waveguiding structure [18]. This is a reasonable approach for many waveguide structures, but the applicability of the concept depends on the geometry of the background “at infinity”. As we saw in the preceding section, our background line constitutes a more general formulation of the same concept.

#153125 - $15.00 USD Received 18 Aug 2011; revised 4 Nov 2011; accepted 4 Nov 2011; published 14 Nov 2011

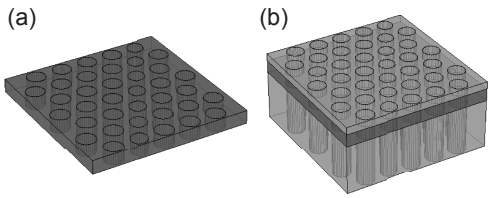

Fig. 4. Planar PhC waveguides. (a) membrane-type; (b) substrate-type.

3.1. The background line of PhC waveguides

First, we will briefly address the membrane-type PhC structures, surrounded by a homogeneous low-index material. It can be a PhC slab waveguide as in Fig. 4(a), a line defect waveguide, or a PhC microcavity device. For the simple PhC slab, the background at infinity is composed of the homogeneous material on top and below, since there is no lateral confinement. If defect modes are considered, then the lateral field decay is guaranteed by the PhC, as long as the device is operated within the photonic bandgap. In this sense, the background line corresponds to the light line for the membrane-type structures, which confirms the common practice of using this line as a separatrix between guided (or localized in the case of a point defect) and non-guided modes.

Now we turn to the case of a substrate-type PhC waveguide with large h_{top} and h_{bot} (as defined in Fig. 1(a)), the background is formed (if h_{top}, $h_{\mathrm{bot}} \to \infty$) by an infinitely extended 2D line defect PhC waveguide. The set of background modes is a lot more complicated than it was for the BRWG system studied above. To numerically determine the background line, the modes of the line defect waveguide have to be simulated for all propagation directions. All oscillating modes of the background system have to be included into a band diagram which is projected onto the core axis of the full system. In Fig. 5 we consider a single line defect (W1) PhC waveguide based on an InP/InGaAsP/InP layer structure, which resembles the BRWG of Fig. 1(a) in terms of geometry of the cross-section. The lateral mode confinement is no longer given by a homogeneous material but by a PhC structure of triangular geometry and an r/a ratio of 0.34. The simulations are performed by the plane wave expansion method (MPB package [19]), using a supercell as indicated in the inset of Fig. 5. The shaded area in Fig. 5 comprises all oscillating modes of the background (regardless of parity). The lower bound of the shaded area marks the background line (dashed line). It qualitatively resembles the fundamental mode of a dielectric slab waveguide and clearly lies above the light line of the substrate (solid line). All propagating modes of the full waveguide system (including the core), which are located below the background line, are guided modes. Contrary to common belief, this also applies to those modes, which are situated between the light line of the substrate and the background line. For the task of designing a waveguide with guided modes, the position of the background line has to be taken into account *instead* of the substrate light line.

We are looking for guided modes which lie below the background line and inside the photonic bandgap. As a coarse reference, the TE bandgap of the underlying PhC is indicated in Fig. 5 by two horizontal lines. Although the background line is still far below any potential bandgap mode in the present example, two kinds of strategies can be pursued to design a waveguide that exhibits guided modes within the bandgap. Firstly, the background line can be pushed upward in the dispersion diagram. This can be realized by decreasing the waveguide width (cf. Sec. 3.2). Secondly, the bandgap can be pushed downward by using a core material of higher refractive index (if available) or by modifying the PhC geometry. In Sec. 3.2, one specific design

#153125 - $15.00 USD Received 18 Aug 2011; revised 4 Nov 2011; accepted 4 Nov 2011; published 14 Nov 2011

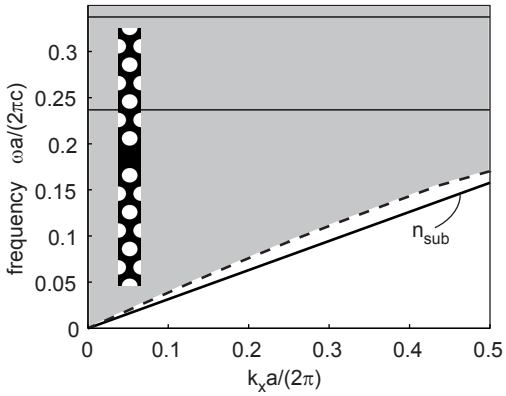

Fig. 5. Simulation of the background line (dashed) of a W1 PhC waveguide. The shaded area indicates the radiation modes of the system (oscillating background modes). The light line of the substrate (n_{sub}) is also indicated (solid). The horizontal lines represent the upper and lower boundaries of the TE bandgap for light propagation in the *x*-*y* plane. The supercell used for the computations is shown as an inset.

approach is briefly addressed. Performing a full structure optimization is beyond the scope of this article. At this stage, it is worth emphasizing that the last word has not been said about losses in substrate-type PhC waveguides. Two open questions remain:

1. Is it possible to design a theoretically loss-free substrate-type PhC waveguide based on realistic materials? The above considerations show that it is not hopeless, but Fig. 5 also shows that for our particular material system it will be very challenging.

2. How much loss do we have for a given mode above the background line? The background line marks the separatrix for guided modes. However, in a typical PhC waveguide, such as the one of Fig. 5, the main component of the Bloch mode is located in the second Brillouin zone [20] and below the background line. Only the Bloch component of the first Brillouin zone lies above the background line, and only that component will contribute to the waveguide loss [21]. The quantitative connection between the strength of this component and the theoretical propagation loss has not been established to our knowledge.

As long as these questions remain open, the final answer cannot be given as to whether or not substrate-type PhC waveguides are viable candidates for a platform of photonic integrated circuits.

3.2. Outlook: vertical current injection for substrate-type PhC devices

So far, we cannot demonstrate the “perfect” design for a substrate-type PhC waveguide. But we can give an outlook of what could be further investigated within the framework of InP and related materials. To illustrate the practical relevance of the background line concept for PhC-based devices, we present the example of an electrically pumped PhC waveguide. The proposed device geometry is depicted in Fig. 6(a). The figure shows a scanning electron microscopy (SEM) image of an InP/InGaAsP/InP layer structure with an additional InGaAs cap layer on top. The quaternary layer could host one or several quantum wells providing for optical gain (not the case here). The sample was etched in hydrochloric acid to remove the InP claddings; only a narrow post remains on both sides of the guiding layer. The background of this system can be thought of as a narrow vertical slab waveguide of InP surrounded by air.

#153125 - $15.00 USD Received 18 Aug 2011; revised 4 Nov 2011; accepted 4 Nov 2011; published 14 Nov 2011

The computed dispersion curves of the fundamental TE modes of this idealized background are shown in Fig. 6(b) for various widths of the posts. For decreasing post width, the background line approaches the light line of air, which gives a lot of theoretical design freedom for the PhC waveguide. A loss-free device is theoretically possible; and in terms of fabrication, the proof of principle is given in Fig. 6(a). However, the narrower the posts are, the less efficient the vertical current injection will be. Furthermore, due to fabrication imperfections (shape of the holes and the contact posts, lattice disorder, etc.), the propagation losses in a real device will always be finite. For an active device, a trade-off between optical and electrical performance will have to be made, taking into account the available fabrication capabilities.

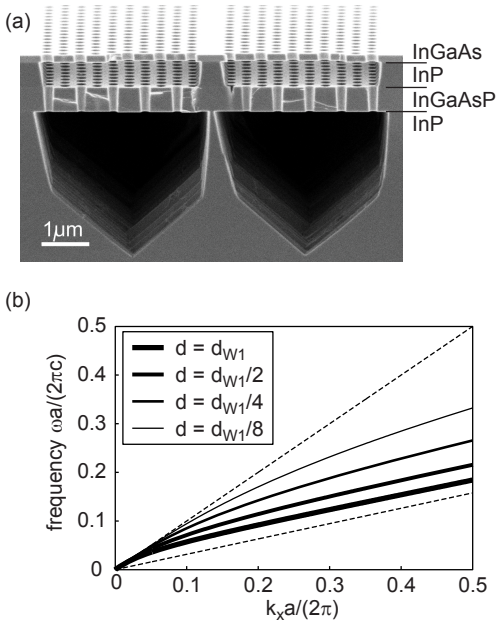

Fig. 6. (a) Prototype W1 PhC waveguide for electrically pumped active devices; (b) Dispersion curves of the fundamental TE modes of four symmetric dielectric slab waveguides of different width d. The widths are indicated in units of $d_{W1} = 458$ nm, which corresponds to the width of a W1 waveguide with $a = 435$ nm and $r/a = 0.34$. The waveguides are composed of InP and air and serve as an approximation of the background system of the waveguide shown in (a). The dashed lines are the light lines of air (upper line) and InP (lower line).

4. Conclusion

A new view on the dispersion diagram of a buried rectangular waveguide was presented. The separatrix between guided and non-guided modes was identified to be given by the fundamental modes of the slab waveguide that forms the background of the structure at infinite distances from the core. The new separatrix is termed “background line” and replaces the conventional “light line”. The background line concept was applied to deeply etched substrate-type PhC waveguides; and it was inferred that, contrary to conventional wisdom, there can be guided modes above the light line of the substrate. This gives some new freedom for the design of theoretically loss-free substrate-type PhC devices. However, for waveguides based on a InP/InGaAsP/InP layer structure, the design of loss-free propagation remains a challenge. For

#153125 - $15.00 USD Received 18 Aug 2011; revised 4 Nov 2011; accepted 4 Nov 2011; published 14 Nov 2011

many other waveguide geometries, such as optical fiber or the membrane-type PhC, the background line falls on the light line and the new concept leads to the same conclusions as the standard light line argument.

Acknowledgment

The authors would like to thank Prof. Dr. C. Hafner (Electromagnetic Fields and Microwave Electronics Laboratory, ETH Zurich) for fruitful discussions.

#153125 - $15.00 USD Received 18 Aug 2011; revised 4 Nov 2011; accepted 4 Nov 2011; published 14 Nov 2011